

RESEARCH ARTICLE

10.1029/2018GC007883

Key Points:

- Dissolved Cr (III) accounts for 48–54% total dissolved Cr in the ETNP region
- The offset between dissolved $\delta^{53}\text{Cr(III)}$ and $\delta^{53}\text{Cr(VI)}$ is relatively constant and is uncorrelated with dissolved O_2 concentration
- More species-dependent Cr isotope data are needed to better constrain Cr isotope fractionation factors in the global ocean

Supporting Information:

- Supporting Information S1
- Data Set S1

Correspondence to:

X. Wang,
xwang@southalabama.edu

Citation:

Wang, X., Glass, J. B., Reinhard, C. T., & Planavsky, N. J. (2019). Species-dependent chromium isotope fractionation across the eastern tropical North Pacific oxygen minimum zone. *Geochemistry, Geophysics, Geosystems*, 20, 2499–2514. <https://doi.org/10.1029/2018GC007883>



Received 8 AUG 2018

Accepted 27 APR 2019

Accepted article online 7 MAY 2019

Published online 30 MAY 2019

Species-Dependent Chromium Isotope Fractionation Across the Eastern Tropical North Pacific Oxygen Minimum Zone

Xiangli Wang^{1,2} , Jennifer B. Glass³ , Chris T. Reinhard³, and Noah J. Planavsky⁴

¹Department of Marine Sciences, University of South Alabama, Mobile, AL, USA, ²Dauphin Island Sea Lab, Dauphin Island, AL, USA, ³Georgia Institute of Technology, Atlanta, GA, USA, ⁴Yale University, New Haven, CT, USA

Abstract The stable chromium (Cr) isotope system is an emerging paleoredox proxy. Interpretation of sedimentary and seawater $\delta^{53}\text{Cr}$ ($^{53}\text{Cr}/^{52}\text{Cr}$ relative to SRM 979) hinges on our understanding of the isotopic fractionations during Cr sequestration from seawater to sediments. Seawater $\delta^{53}\text{Cr}$ values reported thus far are for total dissolved Cr. This study reports the $\delta^{53}\text{Cr}$ of both dissolved Cr (III) and dissolved Cr (VI) across the oxygen minimum zone in the eastern tropical North Pacific off Manzanillo, Mexico. Dissolved Cr (III) accounts for 48% to 54% total dissolved Cr in this region. There are no correlations between O_2 and Cr concentrations, or O_2 concentrations and $\delta^{53}\text{Cr}$ throughout the water column. The $\delta^{53}\text{Cr}$ of Cr (III) is lower than that of Cr (VI) by a relatively constant offset ($0.42 \pm 0.15\%$, 1σ , $n = 5$) and is also uncorrelated with dissolved O_2 concentration. These observations provide part of the foundation for using $\delta^{53}\text{Cr}$ of the authigenic Cr in organic-rich shales to reconstruct seawater $\delta^{53}\text{Cr}$. A survey of growing literature Cr concentration and $\delta^{53}\text{Cr}$ data suggests that the Cr isotope fractionation factor in the global ocean is likely more complex than previously thought. More future species-dependent Cr isotope studies could shed new light on the biogeochemical processes controlling the oceanic Cr isotope fractionation.

Plain Language Summary The chromium isotope system is widely used to reconstruct the Earth's oxygenation history. However, the behavior of the isotope system under low-oxygen conditions in the modern ocean is still poorly understood. It is well known that both oxidized and reduced Cr species coexist in seawater, but all previous studies only measured total Cr isotope compositions. In this study, we sampled seawater from the oxygen minimum zone (OMZ) in the eastern tropical north Pacific region, separated different Cr species, and measured their isotopic compositions. We found that the offsets in isotope compositions between oxic and reduced Cr species are relatively small compared to intrinsic isotope fractionations determined in laboratory experiments, and the offsets are not correlated with dissolved oxygen concentrations. Our species-specific Cr isotope data from the eastern Pacific OMZ, and some previous total Cr isotope data from eastern Atlantic OMZ, do not conform to a global isotope fractionation factor. Therefore, more species-specific Cr isotope data are needed to better understand Cr isotope behavior in the ocean.

1. Introduction

The chromium (Cr) isotope system is an emerging paleoredox proxy that has been recently widely used to reconstruct redox shifts in paleoceans (Albut et al., 2018; Canfield et al., 2018; Cole et al., 2016; Crowe et al., 2013; Frei et al., 2009; Gilleaudeau et al., 2016; Holmden et al., 2016; Huang et al., 2018; Planavsky et al., 2014; Wang, Planavsky, Reinhard, et al., 2016; Wei et al., 2018). However, biogeochemical cycling and isotope fractionation of Cr in the modern ocean is still poorly understood. Particularly, understanding of the Cr redox transformations and associated isotope fractionations through oxygen minimum zones (OMZs) is still in the nascent stage (Goring-Harford et al., 2018; Moos, 2018; Moos & Boyle, 2018). Part of the reason for variable previous observations is likely a lack of species-specific Cr isotope data. This study provides the first attempt to investigate species-specific Cr isotope fractionation through the OMZs in the Eastern Tropical North Pacific (ETNP) region.

Chromium is a transition metal that occurs in the trivalent and hexavalent oxidation states in aquatic environments (Richard & Bourg, 1991). At circum-neutral pH, Cr is thermodynamically stable in the soluble hexavalent state (e.g., CrO_4^{2-} or Cr (VI)) under oxic conditions and in the insoluble trivalent

state (e.g., Cr (OH)₃ or Cr (III)) under anoxic conditions. Rivers are thought to be the major source of dissolved Cr to the ocean (McClain & Maher, 2016), although groundwater fluxes are poorly constrained. Dissolved Cr in river water is primarily derived from the oxidation of insoluble Cr (III) in continental rocks to soluble Cr (VI). This Cr (III) oxidation requires manganese oxides, which in turn requires significant levels of dissolved O₂ (Eary & Rai, 1987). Dissolved Cr (III) has been observed in aquatic systems, presumably due to complexation with dissolved organic matter (Buerge & Hug, 1998; Elderfield, 1970). The primary removal pathway of dissolved Cr from seawater is Cr (VI) reduction and burial as Cr (III) in reducing sediments (Reinhard et al., 2013). Because of its redox-dependent solubility, Cr concentrations in sedimentary rocks have been used to reconstruct fluctuating marine O₂ levels through time (Reinhard et al., 2013).

Stable Cr isotope composition ($\delta^{53}\text{Cr}$, expressed in $^{53}\text{Cr}/^{52}\text{Cr}$ against the NIST SRM979 standard) is potentially a more robust redox proxy than Cr concentration. Oxidation of Cr (III) to Cr (VI) is believed to be necessary for generating appreciable $\delta^{53}\text{Cr}$ fractionation in natural samples, given that there is a narrow range of $\delta^{53}\text{Cr}$ values in igneous rocks (Bain & Bullen, 2005; Døssing et al., 2011; Ellis et al., 2002; Kitchen et al., 2012; Schauble et al., 2004; Schoenberg et al., 2008; Wang et al., 2015). However, in contrast to this traditional view, ligand-promoted Cr (III) dissolution can induce large Cr isotope fractionations (Babechuk et al., 2018; Saad et al., 2017). Despite the potential for nonredox-dependent fractionations, the majority of Archean and Proterozoic sediments have crustal $\delta^{53}\text{Cr}$, which is interpreted as evidence for insufficient atmospheric O₂ for manganese oxides to mediate Cr (III) oxidation by O₂ (Cole et al., 2016; Frei et al., 2009; Planavsky et al., 2014; Qin & Wang, 2017; Wille et al., 2013). Based on this framework, the $\delta^{53}\text{Cr}$ composition of marine sedimentary rocks has been used to broadly track the evolution of atmospheric O₂ (Albut et al., 2018; Cole et al., 2016; Crowe et al., 2013; Frei et al., 2009; Planavsky et al., 2014).

Early $\delta^{53}\text{Cr}$ paleoredox studies focused on banded iron formations and ironstones (Crowe et al., 2013; Frei et al., 2009; Planavsky et al., 2014). Unfortunately, these deposits are rare and discontinuous through geological history (Bekker et al., 2010). Although carbonate is more geologically common, carbonate $\delta^{53}\text{Cr}$ can be influenced by various biological effects because carbonate formation is typically biologically controlled (Farkaš et al., 2018; Frei et al., 2018; Pereira et al., 2015; Wang, Planavsky, Hull, et al., 2016). Although experiments have shown that abiogenic carbonate may faithfully record the $\delta^{53}\text{Cr}$ of the coexisting solution (Rodler et al., 2015), diagenetic alteration can easily alter primary geochemical trace element and isotopic signatures in carbonate rocks (Hood et al., 2018). Therefore, interpreting carbonate $\delta^{53}\text{Cr}$ requires great caution (Gilleaudeau et al., 2016, 2018; Holmden et al., 2016; Pereira et al., 2015; Wang, Reinhard, Planavsky, et al., 2016). Organic-rich siliciclastic sedimentary rocks have much higher Cr concentrations, are more resistant to diagenetic alteration, and can potentially fill temporal gaps in the geologic record (Canfield et al., 2018; Cole et al., 2016; Planavsky et al., 2014; Wang, Planavsky, Reinhard, et al., 2016). However, since organic-rich siliciclastic sediments sequester Cr through reduction, large kinetic isotope fractionation can occur (Døssing et al., 2011; Ellis et al., 2002; Kitchen et al., 2012) and needs to be constrained in natural marine settings.

Recent studies revealed spatial heterogeneity of total $\delta^{53}\text{Cr}$ in global seawater (Bonnand et al., 2013; D'Arcy et al., 2016; Economou-Eliopoulos et al., 2016; Farkaš et al., 2018; Frei et al., 2014; Goring-Harford et al., 2018; Holmden et al., 2016; Moos & Boyle, 2018; Paulukat et al., 2015, 2016; Pereira et al., 2015; Scheiderich et al., 2015). However, surprisingly, no appreciable anomaly in total dissolved Cr and total $\delta^{53}\text{Cr}$ has been found in low-O₂ waters (O₂ > 13 μM) of the eastern subtropical Atlantic (Goring-Harford et al., 2018) and ETNP region (Moos & Boyle, 2018). Although some studies have suggested that kinetic isotopic fractionation during Cr reduction in seawater can be muted (Gueguen et al., 2016; Reinhard et al., 2014), direct measurement of $\delta^{53}\text{Cr}$ composition of Cr (VI) and Cr (III) in seawater is still lacking. Quantifying the $\delta^{53}\text{Cr}$ fractionation during reduction of Cr (VI) to Cr (III) in the ocean is key to using sedimentary $\delta^{53}\text{Cr}$ to infer seawater $\delta^{53}\text{Cr}$ for reconstructing changing ocean redox. This study investigated Cr (III)-Cr (VI) speciation and associated isotope effects across the ETNP OMZ.

2. Site Information

The ETNP contains the largest OMZ in the world (Cline & Richards, 1972; Karstensen et al., 2008; Richards, 1970; Wright et al., 2012). It is a part of an O₂-deficient water layer (100–200- to 800–900-m depth) covering

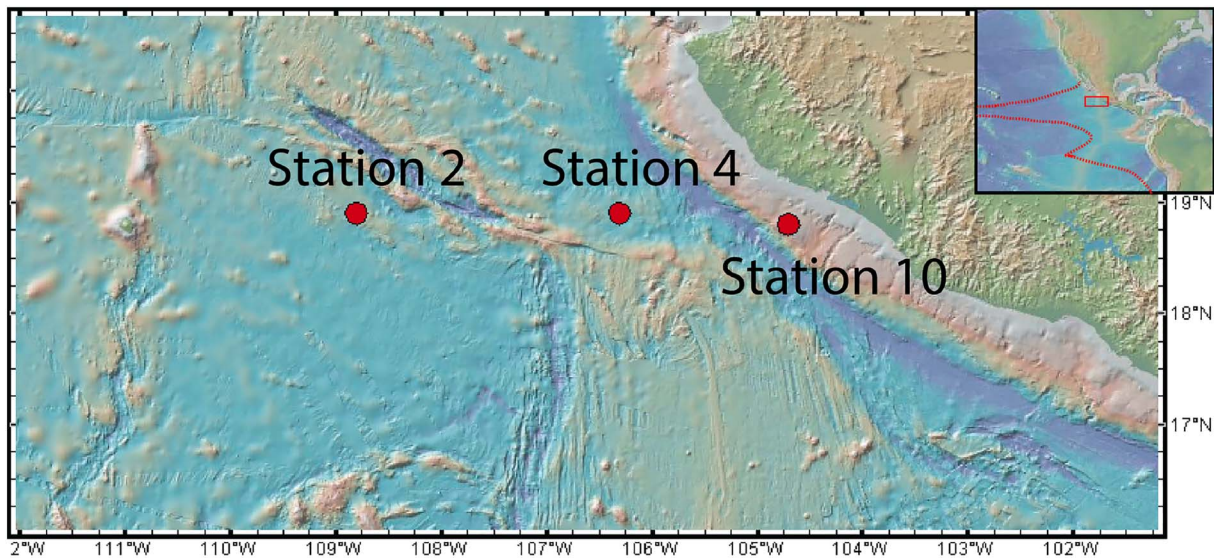


Figure 1. Station locations. The red dashed line in the inset demarcates the approximate border of the eastern tropical North Pacific oxygen minimum zone at 200 dbar (Stramma et al., 2010). Depth of stations: station 2 = 3,400 m, station 4 = 3,300 m, and station 10 = 1,400 m.

the west coast of Central and South America from $\sim 20^{\circ}\text{N}$ to $\sim 15^{\circ}\text{S}$ (Karstensen et al., 2008). Surface water is supplied by the cold California Current, upwelling of nutrient-rich North Atlantic Deep Water, and the warm eastward equatorial countercurrent (Fiedler & Talley, 2006). Intermediate water is supplied by low-salinity North Intermediate Water. Water leaves the ETNP through the westward north equatorial current. Oxygen is depleted by upwelling-related high productivity, thermal stratification, and poor ventilation. The threshold dissolved O_2 concentration that defines the OMZ is debated ($0.03\ \mu\text{M}$, Cline & Richards, 1972; $4.45\ \mu\text{M}$, Karstensen et al., 2008; $20\ \mu\text{M}$, Wright et al., 2012). However, the exact threshold is not critical in this study. Instead, the term OMZ is simply used here to describe low- O_2 conditions.

Samples for $\delta^{53}\text{Cr}$ analysis were taken from the 30–500-m depth range (Figures 1 and 2) on R/V *New Horizon* cruise NH-1315 in June 2013 offshore Manzanillo, Mexico at station 2 (18.9°N , 108.8°W), station 4 (18.9°N , 106.3°W), and station 10 (18.8°N , 104.7°W ; Glass et al., 2015). The dissolved O_2 concentration drops sharply to $<4\ \mu\text{M}$ at $\sim 70\ \text{m}$ at stations 4 and 10 and at $\sim 120\ \text{m}$ depth at station 2, due to vertical thinning of the OMZ toward the west. Samples were taken from water depths characterized by contrasting physical (temperature and density) and chemical (dissolved O_2 and salinity) properties (Figure 2), in order to maximize the chances of observing Cr isotope fractionation.

3. Analytical Methods

3.1. Overview of Procedures

Water samples were taken with a 30-L GoFlo (General Oceanics) or 20-L Niskin-X bottles with external Teflon-coated springs (Ocean Test Equipment) on a plastic-coated hydrowire from depths of 30–500 m. Sampling bottles (GoFlo or Niskin-X) were plumbed with trace metal clean C-flex tubing, and seawater was filtered through acid-cleaned AcroPakTM 200 filters into acid-cleaned LDPE bottles as described in Glass et al. (2015) and following GEOTRACES protocols (Cutter et al., 2010).

As soon as the seawater samples were filtered on the cruise ship, Cr (III) was extracted using precleaned Chelex-100 resin (Rue et al., 1997). The Chelex resin containing Cr (III) was then filtered from seawater, dried in a clean environment (plastic hood on the cruise ship under a HEPA filter), and stored in clean bottles for later processing. The remaining seawater containing Cr (VI) was frozen at -20°C for subsequent Cr (VI) extraction in the lab using an iron coprecipitation method. Purified Cr was dissolved in 0.75 N HNO_3 and measured for $\delta^{53}\text{Cr}$ on a Neptune Plus MC-ICP-MS using double spike technique to correct mass bias during sample preparation and instrument analysis, following protocols described in Wang, Planavsky, Reinhard, et al. (2016).

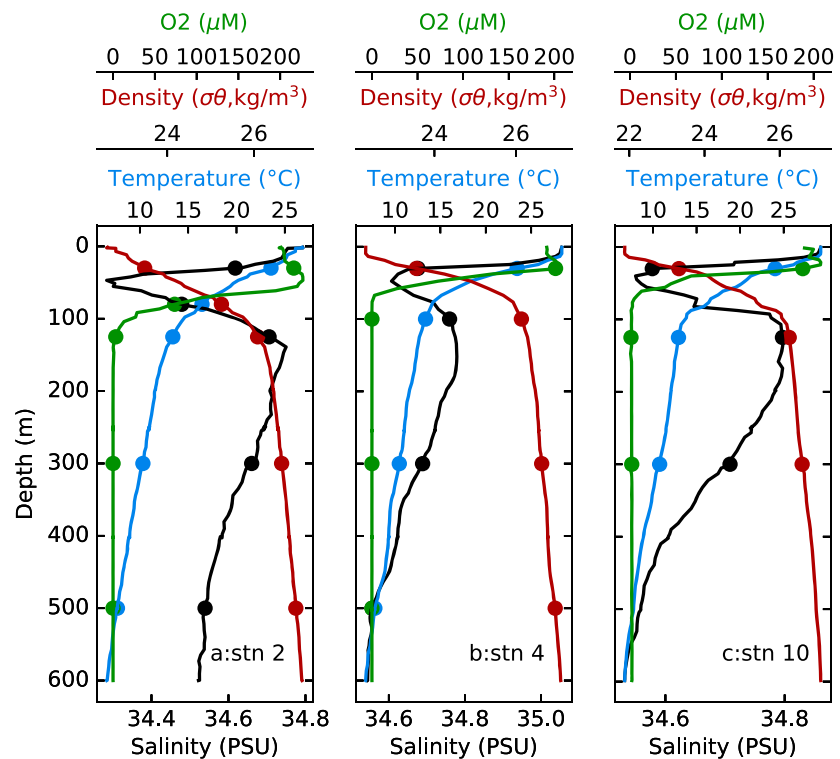


Figure 2. Density (red), salinity (black), temperature (blue), and dissolved oxygen (green) data at stations 2 (a), 4 (b) and 10 (c). Points on curves denote sampling depths. Data available in the supporting information.

3.2. Using Chelex-100 Resin to Extract Cr (III)

The Chelex[®] 100 resin (50–100 mesh) was obtained from Sigma Aldrich (Cat.# C7901-50g). Our batch of resin had $\sim 25 \pm 3$ ng (2SD, $n = 3$) Cr and needed cleaning to reduce the blank. Cleaning with 7.5 N HNO₃ and Milli-Q water reduced blank to 0.25 ng. The cleaned resin slush (equivalent to 3 g of dry resin) suspended in pure water was mixed with 2 L filtered seawater at natural seawater pH for 6–12 hr in pre-cleaned polyethylene terephthalate glycol bottles (agitated gently at room temperature). The Chelex resin containing Cr (III) was then filtered, dried, and brought back to the lab and treated with 7.5 N HNO₃ overnight at 130 °C to release Cr.

The pH of the sample greatly influences the yield of Cr (III) and cross contamination from Cr (VI). To test Cr yields and potential isotope fractionation during Chelex-100 extraction, we doped artificial seawater (composition following Nordstrom et al., 1979) with SRM979 standards in the form of Cr (III) and Cr (VI). The Cr blank of the artificial seawater used was ~ 1.1 ng. The pH was adjusted to 4, 6, and 8 with HCl and NH₄OH after adding the Cr standard and mixed with Chelex-100 resin. The results (Table 1) show that at pH 4, the yields for both Cr (III) and Cr (VI) are 100%. As pH increases to 6 and 8, the yields for both Cr (III) and Cr (VI) decrease, with Cr (VI) decreasing faster. For example, at pH 8, Chelex-100 resin extracted $\sim 80\%$ of Cr (III) from seawater while taking only 8% Cr (VI). The incomplete recovery of Cr (III) at pH 8 does not fractionate Cr (III) isotopes (Table 1), whereas the extracted 8% Cr (VI) is fractionated (0.9‰; Table 1). The error introduced by cross contamination is similar to the analytical error (supporting information). Therefore, we chose to extract Cr (III) at natural seawater pH to achieve a sufficiently high Cr (III) yield while keeping Cr (VI) contamination low. This pH choice is consistent with a previous study (Rue et al., 1997), although Rue et al. reported $>95\%$ recovery of Cr (III) at natural seawater pH. We report uncorrected $\delta^{53}\text{Cr}$ values for discussion in the remainder of this paper for two reasons: (1) The isotope fractionation factor of Cr (VI) during Chelex-100 extraction has a large uncertainty and probably varies between real seawater and artificial seawater, and (2) the correction is close to the analytical precision.

Table 1
Chromium Concentration and $\delta^{53}\text{Cr}$ Results for Validating Methods Employed in This Study

Test sample name	Purpose of test	Cr concentration, mass, and yield	$\delta^{53}\text{Cr}$
New Chelex-100 (3 g)	Blank Cr	25 ± 3 ng ($n = 3$)	0.1 ± 0.2‰
Cleaned Chelex-100 (3 g)	Blank Cr	0.25 ng ($n = 1$)	
Artificial seawater (ASW)	Blank Cr	1.1 ng	
Acid-cleaned AcraPak filter	Blank Cr	0.23 ± 0.09 ng ($n = 4$)	
pH = 4	SRM979 Cr (III)	Cr (III) yield	100%
	SRM979 Cr (VI)	Cr (VI) yield	100%
pH = 6	SRM979 Cr (III)	Cr (III) yield	99 ± 1%
	SRM979 Cr (VI)	Cr (VI) yield	45 ± 3%
pH = 8	SRM979 Cr (III)	Cr (III) yield	80 ± 3%
	SRM979 Cr (VI)	Cr (VI) yield	8 ± 2%
OSIL seawater	Test accuracy	147.8 ng/kg	0.86 ± 0.25‰
SRM 3112a	Test reproducibility		−0.05 ± 0.07‰

We also note that Chelex-100 resin is not suitable for reuse for two reasons: (1) the strong acid and high temperature required to release Cr from the resin compromise the integrity of the resin, leading to low future yields; (2) if a lower temperature is chosen to release Cr from the resin, potential significant relict Cr can remain on the resin, leading to contamination of the next-round samples.

3.3. Iron Coprecipitation Method

Chromium (VI) was extracted from the remaining seawater by coprecipitation with $\text{Fe}(\text{OH})_2$ (Bonnand et al., 2013; Cranston & Murray, 1978; Scheiderich et al., 2015). The $\text{Fe}(\text{OH})_2$ was derived from ammonium $\text{Fe}(\text{II})$ sulfate hexahydrate (99.997% trace metals basis, Sigma Aldrich, Cat. #203505-25G). The pH of the seawater was adjusted to 9–10 with SeaStar ammonium hydroxide, then ammonium $\text{Fe}(\text{II})$ solution was added to the sample to form $\text{Fe}(\text{OH})_2$. The suspension was placed on a shaker for 2 hr and then allowed to stand overnight to allow the precipitate to settle down to the bottom of the bottle. The majority of the clear solution was siphoned off, leaving only ~50 ml at the bottom of the bottles. The 50-ml remaining suspension was then centrifuged at 4,000 rpm for 4 min. The solid material after centrifugation was dissolved in 6 N HCl.

3.4. Addition of Cr Double Spike

A ^{50}Cr - ^{54}Cr double spike technique was used to correct for potential isotope fractionation during sample preparation and mass bias during instrument measurement. Adding the proper amount of double spike requires knowledge of Cr concentrations in samples. Trace element concentrations in the Fe extract and Chelex resin extract were measured on a Thermo Finnigan Element XR ICP-MS, with typical precisions better than 5% on Cr. Ideally, the double spike should be added to samples prior to any sample preparation procedures. In this project, for Cr (VI) we were able to add double spike right before the Fe coprecipitation procedure. Chromium (VI) concentration was estimated by processing 50-mL seawater samples using the same coprecipitation method described above. However, for Cr (III) we were only able to add double spike after the Chelex extraction, because of limited logistics on the cruise ship. However, this approach does not influence the isotopic determination for Cr (III), as discussed above.

Based on measured Cr concentrations, the proper amount of the double spike was added as Cr (III) to the Chelex resin extract and as Cr (VI) to seawater samples to achieve $^{54}\text{Cr}_{\text{spike}}/^{52}\text{Cr}_{\text{sample}}$ of ~0.5 and equilibrated with sample Cr overnight before conducting coprecipitation and ion exchange chromatography. Sample-spike equilibration during reduction and coprecipitation has been demonstrated previously (Scheiderich et al., 2015). Iron was first removed from the Fe extract with AG[®] 1-X8 (100–200 mesh) anion exchange resin (Wang, Planavsky, Reinhard, et al., 2016). Chromium was further purified from Chelex[®] 100 extracts and AG[®] 1-X8 cuts with AG[®] 50W-X8 (200–400 mesh) cation exchange resin, following procedures described in Bonnand et al. (2013).

3.5. Procedural Blank, Accuracy, and Precision

Due to the low concentration of Cr in seawater, the blank of the analytical procedure must be very low. Ion exchange chemistries contributed <2 ng Cr blank. Acid-cleaned Chelex resin (7.5 N HNO_3) contributed 0.25 ng

Table 2
Chromium Concentration and $\delta^{53}\text{Cr}$ Data for Cr (VI) and Cr (III) From Eastern Tropical North Pacific Oxygen Minimum Zone Offshore Manzanillo, Mexico

Station	Depth m	Salinity PSU	Dissolved O ₂ μM	Cr (VI)			Cr (III)			$\delta^{53}\text{Cr(VI)}-\delta^{53}\text{Cr(III)}$ ‰	Total $\delta^{53}\text{Cr}$ ‰	Total Cr nM	Nitrate μM	Phosphate μM
				Cr (VI) (nM)	$\delta^{53}\text{Cr(VI)}$ (‰)	2 s.e. (‰)	Cr (III) (nM)	$\delta^{53}\text{Cr(III)}$ (‰)	2 s.e. (‰)					
2 (3,400 m)	30	34.62	216.1	2.50	1.16	0.03							0.05	0.40
	80	34.48	73.74	2.38	1.54	0.04							18.17	2.94
	125	34.71	3.34	2.37	1.67	0.04							17.40	2.14
	300	34.66	0.11	2.58	1.57	0.04							23.17	2.76
	500	34.54	0.10	3.00	1.55	0.03							33.28	3.21
4 (3,300 m)	30	34.68	201.30	2.62	1.65	0.03	2.46	1.23	0.03	0.42	1.45	5.08		0.37
	100	34.76	0	2.31	1.85	0.04	2.75	1.22	0.03	0.63	1.51	5.06	18.86	2.45
	300	34.69	0	2.62	1.67	0.04	2.63	1.27	0.03	0.40	1.47	5.25		
	500	34.56	0	2.92	1.58	0.03							33.20	3.11
10 (1,400 m)	30	34.58	188.10	2.40	1.73	0.04	2.19	1.30	0.03	0.43	1.52	4.59		
	125	34.80	1.19				2.88	1.20	0.03					
	300	34.71	2.02	2.62	1.47	0.03	2.65	1.25	0.03	0.22	1.36	5.27		

Note. Total $\delta^{53}\text{Cr}$ is calculated based on isotope mass balance.

to the Cr blank. Acid cleaning of the AcroPak filter effectively reduced the Cr blank to 0.23 ± 0.09 ng (1σ , $n = 4$). The total Cr blank was <3 ng, or $<5\%$ of sample Cr (~ 100 ng), and thus a blank correction was not performed.

To assess accuracy of our methods, OSIL seawater standard was processed through the Fe coprecipitation method and yielded the same value ($0.86 \pm 0.09\%$ $\delta^{53}\text{Cr}$ and 147.8 ng/kg Cr, $n = 3$) as other studies ($0.96 \pm 0.06\%$ and 157 ng/kg in Scheiderich et al., 2015; $0.97 \pm 0.10\%$ and 161.2 ng/kg in Goring-Harford et al., 2018). Chromium (III) extraction from the OSIL seawater was not attempted because of its long storage time at room temperature, which may have changed the Cr speciation. Reproducibility of $\delta^{53}\text{Cr}$ measurement was 0.07% based on repeated processing and analysis of a commonly used Cr concentration standard NIST SRM 3112a ($-0.05 \pm 0.07\%$, 2SD, $n = 11$), which is consistent with previous measurements (Schoenberg et al., 2008), but the 0.09% reproducibility based on OSIL seawater was used in this paper.

4. Results

Dissolved Cr (VI) and Cr (III) concentrations are nearly equal, in the range of 2.3 to 3.0 nM (Table 2; Figures 3a–3c). At station 4, where we have both Cr (III) and Cr (VI) concentration data for the same water depths, there is a slight decrease in Cr (VI) (9%) and slight increase in Cr (III) (12%) as O₂ decreases in the upper 100 m of the water column (Table 2; Figure 3b). Below 100 m, however, Cr (VI) increases, despite strong depletion in dissolved O₂. At stations 2 and 4, where we had sufficient sampling depths to resolve $\delta^{53}\text{Cr(VI)}$ changes, $\delta^{53}\text{Cr(VI)}$ showed the opposite trend as Cr (VI) concentrations (Figures 3d and 3e). At station 2, $\delta^{53}\text{Cr(VI)}$ increases from $\sim 1.2\%$ at 30 m to $\sim 1.6\%$ after 100 m (Table 2; Figure 3d). At station 4, $\delta^{53}\text{Cr(VI)}$ remained relatively stable at $\sim 1.6\%$ from 30 m down to 500 m except at depth 100 m where the $\delta^{53}\text{Cr(VI)}$ is 1.85% ; $\delta^{53}\text{Cr(III)}$ remains relatively stable (1.22 – 1.27%) from 30 to 300 m, despite large changes in dissolved O₂ (Table 2; Figure 3e). The $\delta^{53}\text{Cr}$ offset between Cr (VI) and Cr (III) at station 4 ranges from 0.40% to 0.63% , with the largest offset at 100 m where O₂ drops sharply (Table 2). Limited data at station 10 suggest that, similar to station 4, $\delta^{53}\text{Cr(VI)}$ has a relatively high value (1.73%) at 30 m and decreases to a relatively low value (1.47%) at 300 m (Table 2; Figure 3f); in contrast, $\delta^{53}\text{Cr(III)}$ stays relatively stable (1.20 – 1.30%) in the same depth range. The $\delta^{53}\text{Cr}$ offset between Cr (VI) and Cr (III) at station 10 is 0.43% at 30 m (same as station 4) and 0.22% at 300 m (smaller than station 4; Table 2). $\delta^{53}\text{Cr(VI)}$ at 30 m varies among three stations, whereas $\delta^{53}\text{Cr(VI)}$ in deeper water, as well as $\delta^{53}\text{Cr(III)}$ throughout the water column, are homogeneous among the stations.

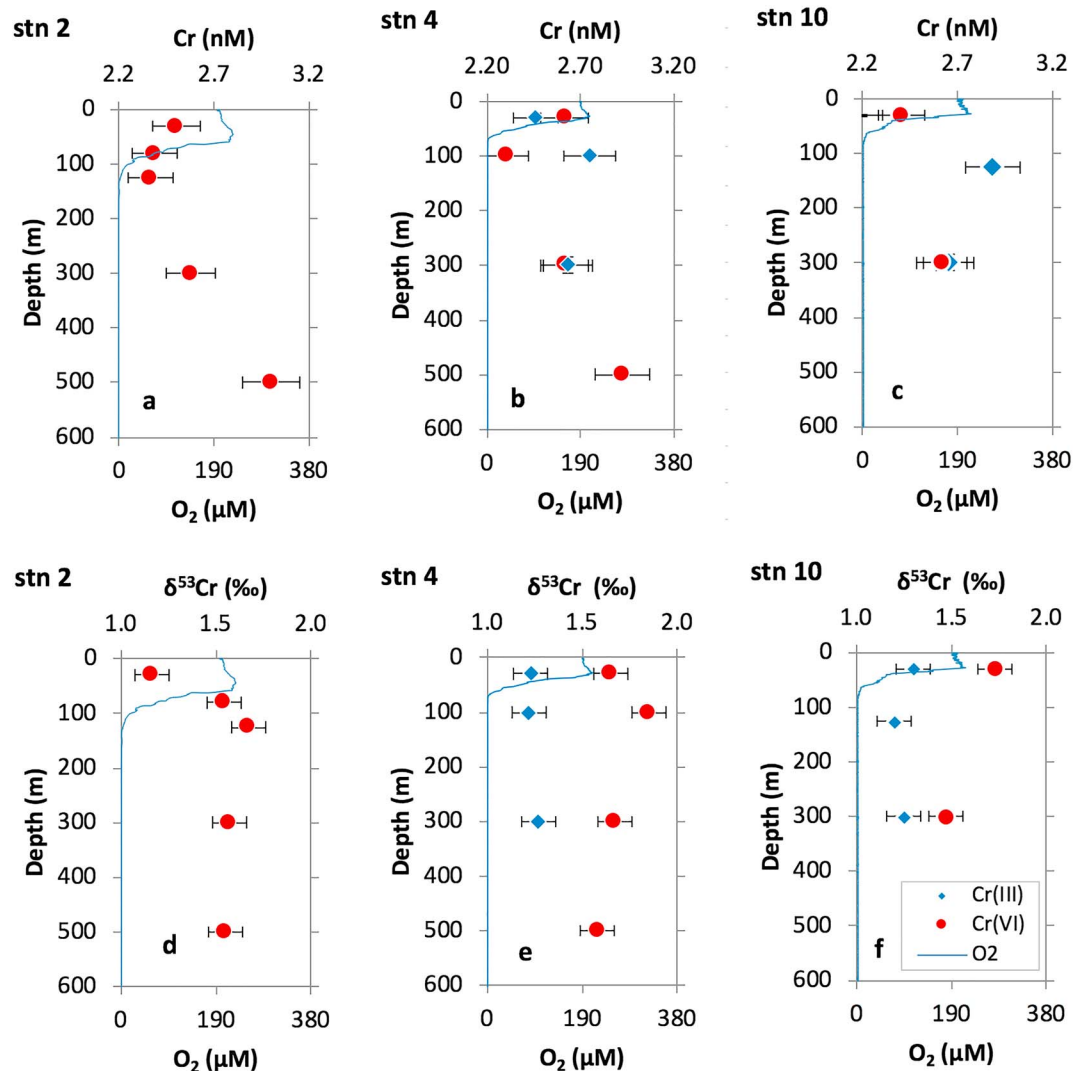


Figure 3. (a, b, c) Dissolved concentrations of Cr (III) (blue rhomboids), Cr (VI) (red circles), and O₂ (blue line) plotted as a function of depth for stations 2, 4, and 10. (d, e, f) δ⁵³Cr(III) (blue rhomboids), δ⁵³Cr(VI) (red circles), and dissolved O₂ (blue line) plotted as a function of depth for stations 2, 4, and 10. Error bars are smaller than symbols.

5. Discussion

5.1. Cr cycling in the ocean

The fate of Cr (VI) within OMZs is not well understood (Goring-Harford et al., 2018; Moos & Boyle, 2018; Murray et al., 1983; Rue et al., 1997). Previous Cr concentration measurements in low-O₂ seawater have reported that up to 50% of reduced Cr (VI) is accounted for by dissolved Cr (III), while the rest is incorporated into particulate matter (Cranston & Murray, 1978; Murray et al., 1983; Rue et al., 1997). In contrast, recent studies in the eastern Atlantic and eastern Pacific OMZs found no significant drawdown of total dissolved Cr (Cr (III) + Cr (VI)) when dissolved O₂ is higher than 13 μM (Goring-Harford et al., 2018; Moos & Boyle, 2018), suggesting either (1) Cr (VI) reduction is not favorable at such O₂ concentrations or (2) Cr (VI) is reduced to Cr (III) but Cr (III) is not scavenged. The high dissolved Cr (III) shown by our data appears to support the second scenario, and the Cr (III) produced is likely complexed by dissolved organic matter (e.g., Nakayama et al., 1981; Saad et al., 2017). Indeed, Glass et al. (2015) reported that dissolved organic ligands with strong conditional stability constants are present at excess at the same stations as those investigated in this study.

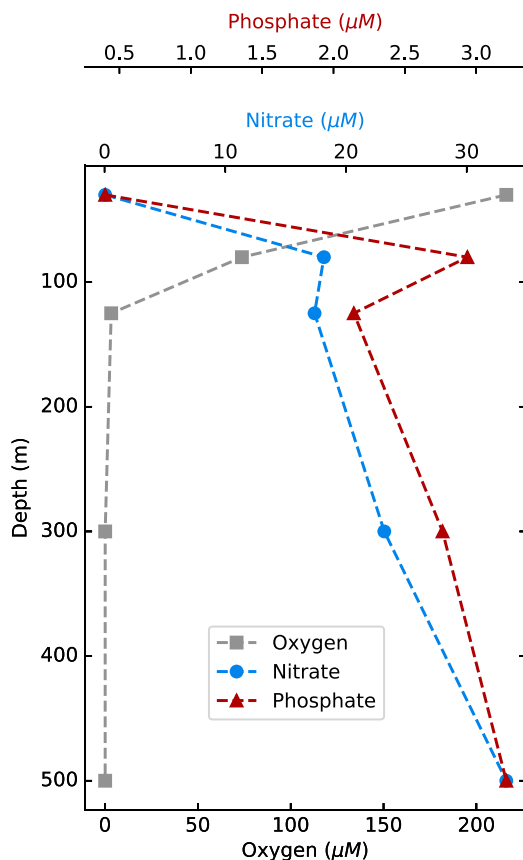


Figure 4. Phosphate (red triangles), nitrate (blue circles), and dissolved O_2 (grey squares) depth profiles for station 2. Similar profiles were observed at stations 4 and 10. Data from Glass et al. (2015).

Murray et al. (1983) and Rue et al. (1997) studied the same general ETNP region as our study, yet their reported dissolved Cr (III) concentrations (up to 0.7 nM) are much lower than our values (2.2–2.9 nM). Such discrepancies could be explained by seasonal variability of dissolved Cr (III). Rue et al. (1997) stations were sampled in November 1981 and 1982, Murray et al. (1983) stations in February 1978, and our stations were sampled in June 2013. Indeed, Connelly et al. (2006) reported that in the Sargasso Sea region of the North Atlantic ocean, dissolved Cr (III) in March (>4 nM) is much higher than other months (June, September, November, and January), likely related to productivity. Excess dissolved organic matter was observed by Glass et al. (2015), which could have allowed more Cr (III) to stay dissolved.

Chromium (VI) reduction has been suggested to be biologically mediated (Achterberg & van den Berg, 1997; Connelly et al., 2006). The impact of biological processes on Cr (VI) reduction can be informed by comparing Cr (VI) and nutrients (nitrate and phosphate). Nitrate can be used both as an N source and as an energy source, whereas Cr (VI) is only for energy source, and phosphate is only used as a P source. Nitrate at stations 2, 4, and 6 remained relatively high (18 to 33 μM , increasing downward; Glass et al., 2015; Figure 4), except at 30-m depth, where nitrate and phosphate were depleted due to biological uptake in the photic zone. Excluding the 30-m sample, there appears to be a positive correlation between nitrate-Cr (VI) and phosphate-Cr (VI) concentrations (Figures 5a and 5b). There are two possible interpretations for the positive correlation between nitrate and Cr (VI). First, nitrate may compete with Cr (VI) as the terminal electron acceptor during anaerobic respiration (Komori et al., 1989), given that the redox potential of the CrO_4^{2-} -Cr (OH) $_3$ pair (−0.12 V) is very close to that of the NO_3^- - NO_2^- pair (0.01 V; Bratsch, 1989; Fanning, 2000). In other words, when nitrate is high, nitrate may serve as the predominant electron acceptor, thus preventing Cr (VI) reduction. Nitrate reduction is indicated by detected nitrite peaks

at ~250 m for station 2, ~300 m for station 4, and ~100 m for station 10 (Glass et al., 2015). Although Cr (VI) reduction still occurs in the presence of nitrate (Chovanec et al., 2012; Vatsouria et al., 2005), nitrate can slow down Cr (VI) reduction (Komori et al., 1989). Second, low nitrate indicates high biological productivity and high dissolved organic matter that can serve as the electron donor for Cr (VI) reduction (Kitchen et al., 2012), thereby drawing down Cr (VI) concentration. The positive correlation between phosphate and Cr (VI) seems to support the second interpretation discussed above.

The photic zone sample at 30 m is a clear exception to the trends described above. The high Cr (VI) in the photic zone could be due to the abundant O_2 , which may have protected Cr (VI) from being reduced. However, there is no obvious correlation between Cr (VI) or Cr (III) and dissolved O_2 when all samples are considered (Figures 5c and 5d), suggesting that dissolved O_2 do not have a straightforward control on Cr reduction. In summary, we suggest that Cr (VI) reduction is affected by several factors—availability of dissolved O_2 and other competing electron acceptors (e.g., nitrate), as well as biological productivity.

As dissolved O_2 continues to decrease below 125 m, Cr (VI) concentration increases. This phenomenon, which has also been observed previously, is likely caused by diffusion of Cr (VI) from deep oxic water (Cranston & Murray, 1978; Murray et al., 1983; Rue et al., 1997). However, there is no clear relationship between Cr (VI) and dissolved O_2 (Figure 5c). Similarly, limited data do not show a clear relationship between dissolved Cr (III) and dissolved O_2 (Figure 5d). The lack of simple correlation between seawater Cr (VI) and dissolved O_2 implies that Cr concentration in sediments may not be a simple function of dissolved O_2 —whether sediments were deposited on the periphery or core of OMZs will also play a strong role in controlling sediment Cr enrichments.

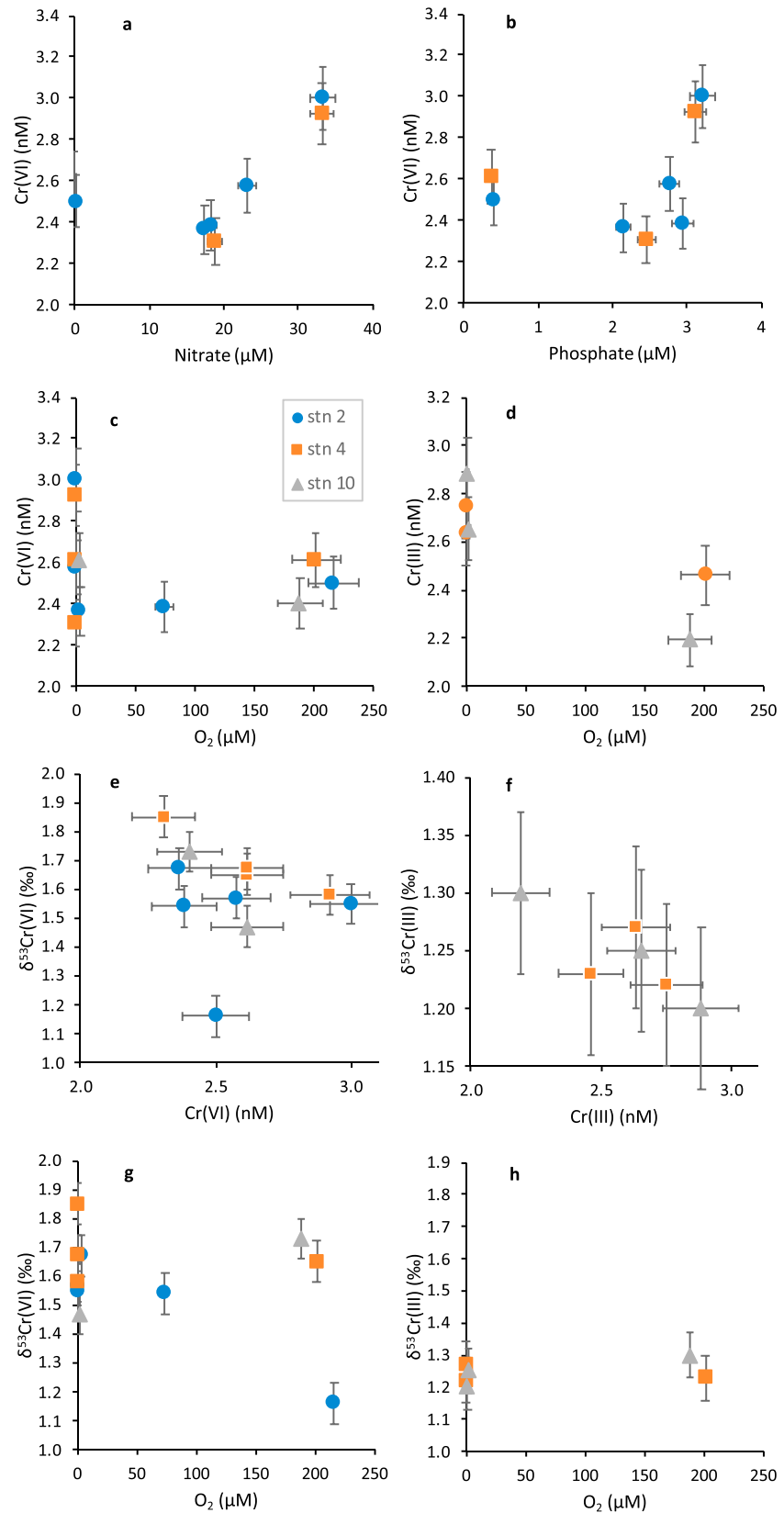


Figure 5. Relationships between Cr concentration, $\delta^{53}\text{Cr}$, dissolved O_2 , nitrate, and phosphate for the three stations (station 2 = blue circles, station 4 = orange squares, station 10 = gray triangles).

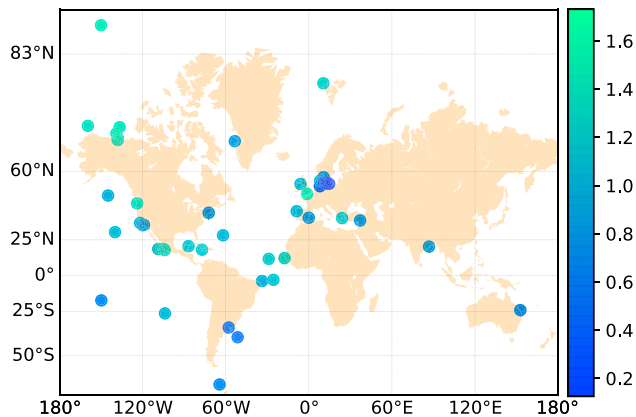


Figure 6. A map showing locations where Cr isotope data (total Cr) are available. The color bar represents the $\delta^{53}\text{Cr}$ value of surface seawater (≤ 100 m). Literature data sources: Bonnard et al. (2013), Frei et al. (2014), Paulukat et al. (2015), Pereira et al. (2015), Scheiderich et al. (2015), D'Arcy et al. (2016), Economou-Eliopoulos et al. (2016), Holmden et al. (2016), Paulukat et al. (2016), Goring-Harford et al. (2018), Moos (2018), and Moos and Boyle (2018).

The fact that significant Cr (VI) can exist in O_2 -depleted water (this study; Rue et al., 1997), or even H_2S -containing water (Cranston & Murray, 1978), suggests that Cr (VI) reduction kinetics in natural reducing marine environments may not be as fast as previously suggested (Reinhard et al., 2014). Therefore, the matching $\delta^{53}\text{Cr}$ between organic-rich shale and Atlantic seawater (Reinhard et al., 2014) may not be a result of quantitative reduction of Cr (VI), but rather a result of small isotope offset between Cr (VI) and Cr (III).

5.2. Relations Between O_2 , Cr Concentration, and $\delta^{53}\text{Cr}$

The $\delta^{53}\text{Cr}$ of Cr (VI) remaining in solution is expected to increase as Cr (VI) is progressively reduced to Cr (III) due to kinetic isotope fractionations during reduction (Døssing et al., 2011; Ellis et al., 2002; Kitchen et al., 2012). However, our data (Figures 5e and 5f; $\text{O}_2 < 4 \mu\text{M}$) and data in Goring-Harford et al. (2018; $\text{O}_2 > 44 \mu\text{M}$) do not show negative correlations between dissolved Cr concentration and $\delta^{53}\text{Cr}$, in sharp contrast to oxic open seawater data (Paulukat et al., 2016; Scheiderich et al., 2015) and low- O_2 seawater ($[\text{O}_2] > 13 \mu\text{M}$) data at the SAFe station (Moos & Boyle, 2018), which is $\sim 3,860$ miles to the northwest of our stations. Because of the nonconclusive relationships between Cr concentration and O_2 , and between $\delta^{53}\text{Cr}$ and Cr concentrations, the relationship

between $\delta^{53}\text{Cr}$ and dissolved O_2 remains elusive (Figures 5g and 5h).

Although seawater Cr concentrations have been measured since 1970s, seawater $\delta^{53}\text{Cr}$ data sets have been unavailable until a few years ago, and most of the data measured so far are for oxic seawaters. These samples come mostly from the North Atlantic Ocean, the northeast Pacific Ocean, and the Arctic Ocean, with small number of samples from other ocean basins (Figure 6). Examination of existing Cr concentration and isotope data that have accompanied dissolved O_2 data reveals lack of correlation between Cr and O_2 and between $\delta^{53}\text{Cr}$ and O_2 , under either oxic ($\text{O}_2 \geq 4 \mu\text{M}$) or suboxic ($\text{O}_2 < 4 \mu\text{M}$) conditions (Figures 7 and 8). The Cr concentration between oxic and suboxic seawater is also indistinguishable (Figure 7g). In contrast, there appears to be distinctive differences between suboxic and oxic species-specific $\delta^{53}\text{Cr}$ values (Figure 8h). For instance, suboxic $\delta^{53}\text{Cr}(\text{VI})$ and suboxic $\delta^{53}\text{Cr}(\text{total Cr})$ are higher than oxic $\delta^{53}\text{Cr}(\text{total Cr})$ and oxic $\delta^{53}\text{Cr}(\text{III})$. However, this is only based on the limited number of species-specific $\delta^{53}\text{Cr}$ data so far. More future species-specific measurements are needed to better constrain the Cr isotope systematics in marine environments.

5.3. Chromium Isotope Fractionation Factor in the Global Ocean

Scheiderich et al. (2015) first reported a linear correlation between $\delta^{53}\text{Cr}$ and natural logarithm of Cr and used it to extract a Rayleigh-type kinetic isotope fractionation factor of -0.8‰ for Cr cycling in the global ocean. Some newer data, such as those from the Baltic Sea, clearly deviate from the trend described in Scheiderich et al. (2015), which has been attributed to freshwater influences (Paulukat et al., 2016). However, after excluding shallow seawater samples, deep water $\delta^{53}\text{Cr}$ data from Eastern Atlantic and Arctic also deviate from the trend (Figures 9b–9d), providing impetuses for further evaluation of the global Cr isotope fractionation factor.

Of special interest is whether OMZ $\delta^{53}\text{Cr}$ data conform to the linear trend observed in Scheiderich et al. (2015). A compilation of OMZ data (colored symbols in Figure 9) shows a more complex relationship between Cr concentration and $\delta^{53}\text{Cr}$. Total Cr isotope data from ETNP suboxic seawater profiles (Moos, 2018; Moos & Boyle, 2018) are consistent with the Rayleigh-type line observed in Scheiderich et al. (2015). However, total seawater $\delta^{53}\text{Cr}$ data from the eastern Atlantic OMZ by Goring-Harford et al. (2018), and species-specific $\delta^{53}\text{Cr}$ data from ETNP reported by this study, only partially fall on the linear trend. Total seawater $\delta^{53}\text{Cr}$ values from the eastern subtropical Atlantic OMZ appear to cluster in two groups: group 1 plots on the Rayleigh-type line, whereas group 2 plots above the line (Figure 8; Goring-Harford et al., 2018). Our species-dependent data overlap well with the eastern subtropical Atlantic OMZ data in Goring-Harford et al. (2018). Furthermore, our Cr (VI) data plot in the same region above the Rayleigh-type line as group 1 in Goring-Harford et al. (2018), whereas our Cr (III) data fall in the same region on the line as group 2 in

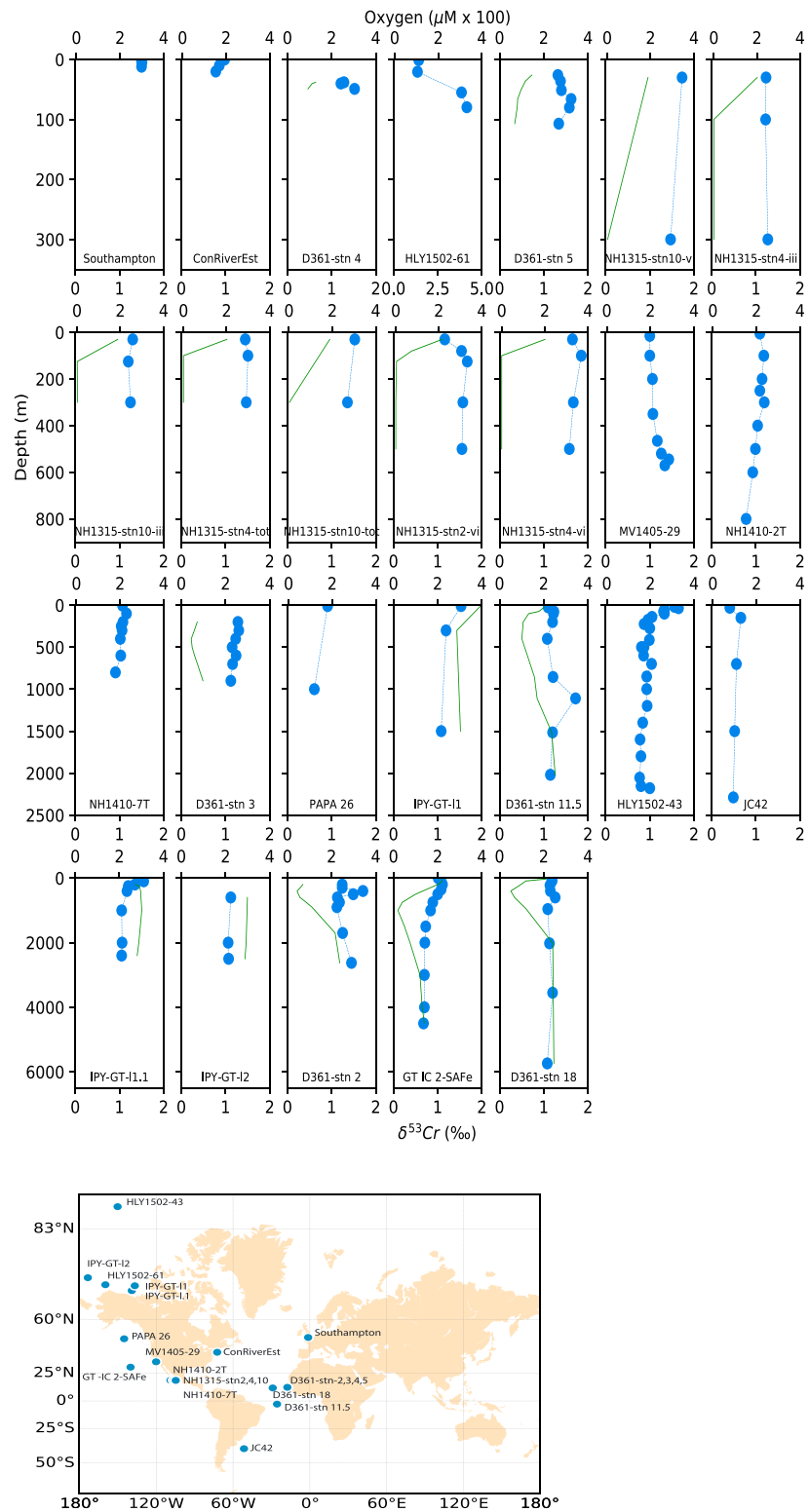


Figure 7. Depth profiles for $\delta^{53}\text{Cr}$ (blue) and dissolved oxygen (green curves). The map shows station locations where depth profile $\delta^{53}\text{Cr}$ data are available. Literature data sources: Bonnand et al. (2013), Scheiderich et al. (2015), Goring-Harford et al. (2018), Moos (2018), Moos and Boyle (2018), and Sun et al. (2019). ConRiverEst = the Connecticut River estuary, III = Cr (III), VI = Cr (VI), tot = total Cr. Notice the different $\delta^{53}\text{Cr}$ scale for station HLY1502-61 (fourth graph on the first row).

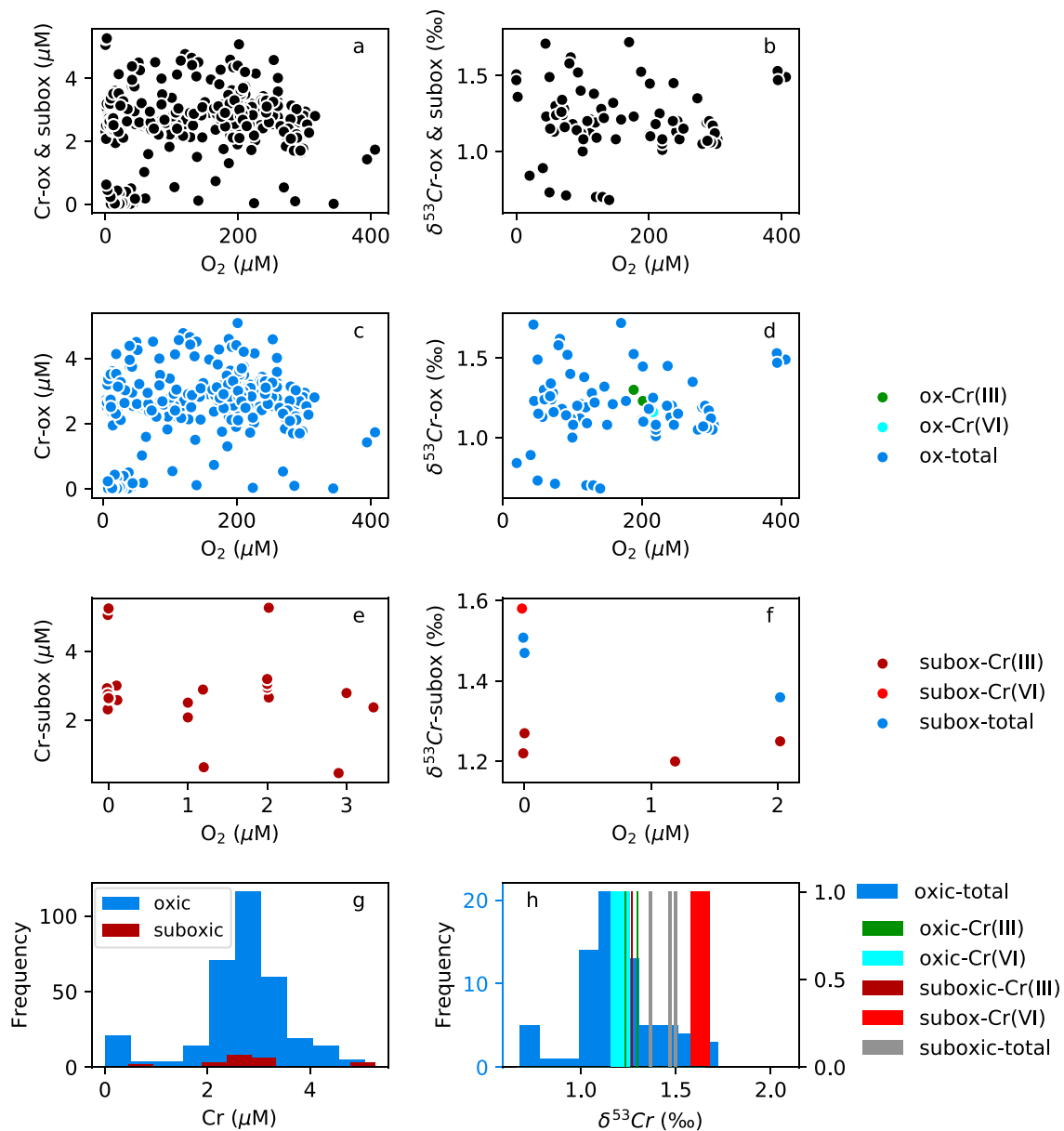


Figure 8. Correlations between Cr concentration and dissolved O₂ concentration (a, c, e) and between $\delta^{53}\text{Cr}$ and dissolved O₂ concentration (b, d, f) under oxic (ox: O₂ \geq 4 μM) and suboxic (subox: O₂ \geq 4 μM) conditions. Literature data sources for Cr concentration (1,075 data points) and $\delta^{53}\text{Cr}$ (92 data points) that have accompanied dissolved O₂ data (Cranston, 1983; Emerson et al., 1979; Goring-Harford et al., 2018; Jeandel & Minster, 1987; Moos, 2018; Moos & Boyle, 2018; Rue et al., 1997; Scheiderich et al., 2015). In Figure 8h, the left y axis is for oxic-total, whereas the right y axis is for all other data.

Goring-Harford (2018). However, the calculated total dissolved Cr data for our samples plot above the previously proposed linear trend (Figure 9).

Moos and Boyle (2018), Moos (2018), and this study reported Cr isotope data from the ETNP region but obtained somewhat different results. At station SAFE, which lies ~2,400 miles northwest of our stations, total Cr concentration reported in Moos and Boyle (2018) is consistent with our species-specific data. However, the total $\delta^{53}\text{Cr}$ data reported in Moos and Boyle (2018) ranges from 0.8‰ to 1.1‰, which is lower than our calculated total dissolved Cr values (Table 2). Given more than a 2,400-mile distance between these locations, such difference in $\delta^{53}\text{Cr}$ may be explained by the highly heterogeneous distribution of Cr isotopes in the modern ocean. In addition, Moos (2018) reported Cr concentration (2.27–3.21 nM) and $\delta^{53}\text{Cr}$ (0.99–1.19‰) at the same station 2 and another station near our station 10 (station 7T in Moos, 2018), which

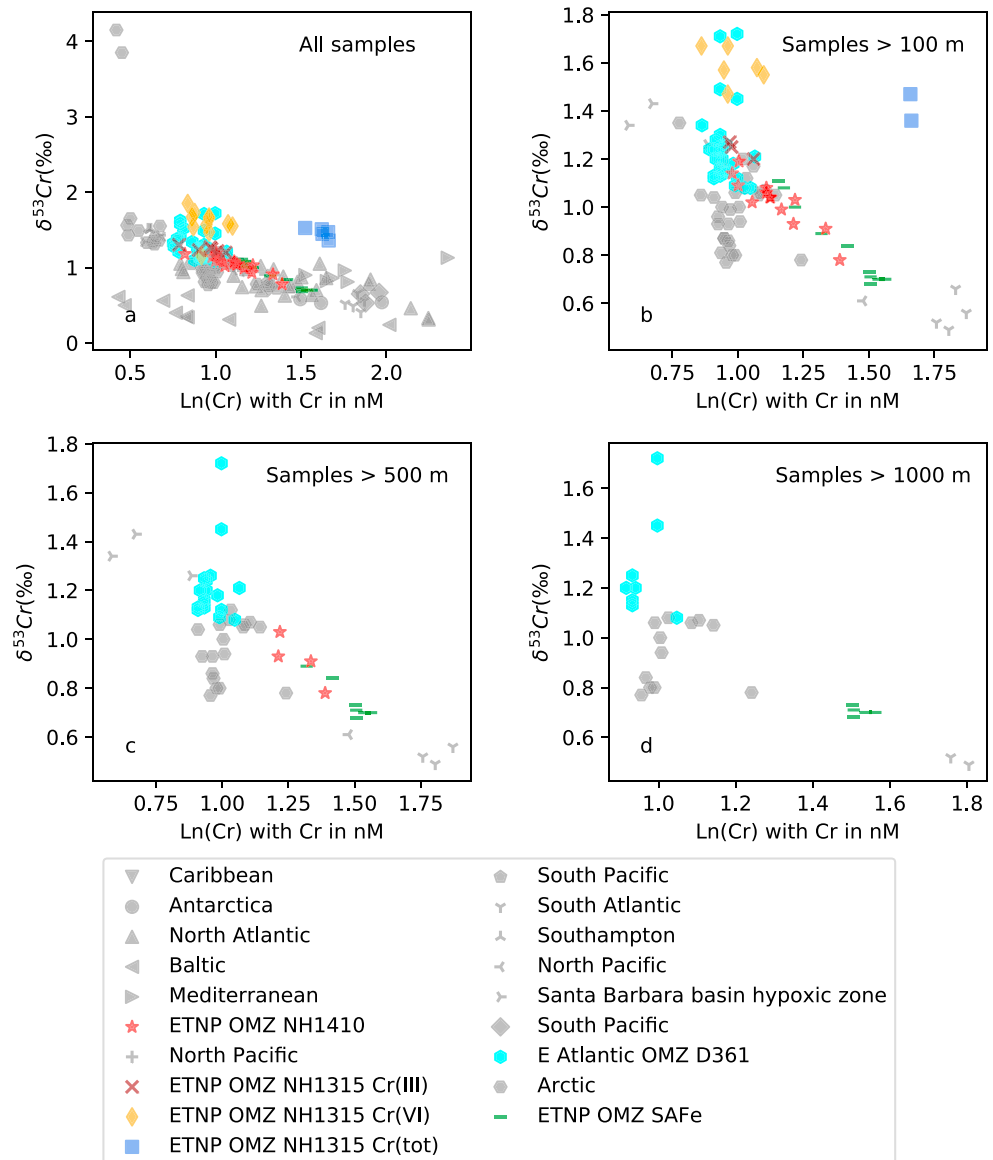


Figure 9. Cross plot of logarithmic Cr concentration (nM) and $\delta^{53}\text{Cr}$ data from this study and previous work. Shallow samples are screened using different depths (100 m for B, 500 m for C, and 1,000 m for D) in order to exclude samples potentially influenced by fresh water (river input in coastal areas and atmospheric rain precipitation in pelagic areas). Colored symbols are for oxygen minimum zone (OMZ) samples (this study; Goring-Harford et al., 2018; Moos & Boyle, 2018; Moos, 2018). Gray symbols represent literature data for oxic seawater (Bonnand et al., 2013; D’Arcy et al., 2016; Farkaš et al., 2018; Holmden et al., 2016; Paulukat et al., 2016; Pereira et al., 2015; Scheiderich et al., 2015; Sun et al., 2019). $\delta^{53}\text{Cr}(\text{tot})$ for this study was calculated based on isotope mass balance of Cr (III) and Cr (VI) data. ETN eastern tropical North Pacific oxygen minimum zone.

are both lower than our values (2.37–2.58 nM Cr (VI) at station 2 and 4.6–5.27 nM total dissolved Cr at station 10). Moos (2018) samples and our samples were collected 1 year apart (June 2013 for our samples and May 2014 for Moos, 2018). Their samples were stored in plastic bottles at pH 2 for >2 years, while our samples were treated with Chelex-100 resin aboard the ship. The lower $\delta^{53}\text{Cr}$ by Moos (2018) than ours is expected because their samples were unfiltered. Sampling time difference and long-term storage may explain the difference in Cr concentrations between these studies.

The observation that our measured $\delta^{53}\text{Cr}$ for “reduced” dissolved Cr (III), but not Cr (VI), agrees with measurements of total $\delta^{53}\text{Cr}$ from more oxic waters appears to be counterintuitive. However, seawater

$\delta^{53}\text{Cr}$ values reported previously were not species-specific. Reduction of Cr (VI) will likely lead to isotopically heavy Cr (VI) and light Cr (III). Therefore, these points plotting above the linear trend (including this study and Goring-Harford et al., 2018) perhaps have Cr (VI) dominating the dissolved Cr pool. The fact that dissolved Cr (III) was not isotopically lighter than previous results, but instead plotted right on the linear trend, can be explained by Cr (III) dominating dissolved Cr. Given that amounting deep seawater $\delta^{53}\text{Cr}$ and Cr concentration data have deviated the originally proposed Rayleigh-type linear trend (Figure 9), we suggest that species-dependent Cr isotope data are needed in future studies to better identify whether there is one or multiple globally applicable Cr stable isotope fractionation factors in the ocean and what mechanisms induce these isotope fractionations. Total Cr isotope data are insufficient for this purpose, because varying proportions of dissolved Cr (III) and Cr (VI) can coexist under different oceanographic conditions, leading to varying total dissolved $\delta^{53}\text{Cr}$ values that may or may not plot on the Rayleigh-type straight line.

5.4. Implications for $\delta^{53}\text{Cr}$ as a Paleoredox Proxy

Interestingly, $\delta^{53}\text{Cr(III)}$ remained uniform at different O_2 concentrations and is generally lower than that of $\delta^{53}\text{Cr(VI)}$ by 0.22–0.63‰ (Table 2). Furthermore, the offset is uncorrelated with dissolved O_2 . This observation has key implications for using the $\delta^{53}\text{Cr}$ of organic-rich siliciclastic sediments. Since Cr (III) is eventually scavenged by sinking particles and buried, the $\delta^{53}\text{Cr}$ of the authigenic component in organic-rich sedimentary rocks may underestimate the concurrent seawater $\delta^{53}\text{Cr}$. However, since the $\delta^{53}\text{Cr}$ offset between Cr (VI) and Cr (III) is relatively constant despite varying O_2 concentration, the authigenic $\delta^{53}\text{Cr}$ in “suboxic” organic-rich shales can potentially be used to broadly track seawater $\delta^{53}\text{Cr}$ evolution regardless of local dissolved O_2 concentrations. Future species-specific Cr isotope studies at other OMZ locations are needed to confirm this O_2 -independent isotope offset between Cr (III) and Cr (VI).

6. Conclusions

We separated Cr (III) and Cr (VI) from seawater samples from the ETNP OMZ and measured their isotopic compositions. Dissolved Cr (III) account for 45–54% of total dissolved Cr (VI). The offset between $\delta^{53}\text{Cr(VI)}$ and $\delta^{53}\text{Cr(III)}$ varies between 0.2‰ and 0.6‰ and is uncorrelated to dissolved O_2 concentrations. This observation, if confirmed by further species-specific studies, provides part of the foundation for using $\delta^{53}\text{Cr}$ of the authigenic Cr in organic-rich shales to reconstruct seawater $\delta^{53}\text{Cr}$. $\delta^{53}\text{Cr(III)}$ data from the ETNP OMZ plot on the $\delta^{53}\text{Cr}$ -Cr trend defined by previous total $\delta^{53}\text{Cr}$ from oxic open seawater, but $\delta^{53}\text{Cr(VI)}$ from the ETNP OMZ plot above the trend. This contrasting behavior between Cr (III) and Cr (VI) warrants collection of more species-specific Cr isotope data to better understand Cr cycling and associated isotopic fractionation factors in the global ocean.

Acknowledgments

This work was supported by the Agouron Institute Postdoctoral Fellowship (AI-FGB31.14.2). We thank Chief Scientist Frank Stewart and the scientific party, officers, and crew for assistance and access to samples on R/V *New Horizon* cruise 1315 supported by the NSF OCE grant 1151698. All data presented in this paper are available in Table 2 and supporting information.

References

- Achterberg, E. P., & van den Berg, C. M. (1997). Chemical speciation of chromium and nickel in the western Mediterranean. *Deep Sea Research Part II: Topical Studies in Oceanography*, 44(3-4), 693–720. [https://doi.org/10.1016/S0967-0645\(96\)00086-0](https://doi.org/10.1016/S0967-0645(96)00086-0)
- Albut, G., Babechuk, M. G., Kleinhanns, I. C., Bengler, M., Beukes, N. J., Steinhilber, B., et al. (2018). Modern rather than Mesoproterozoic oxidative weathering responsible for the heavy stable Cr isotopic signatures of the 2.95 Ga old Ijzermijn iron formation (South Africa). *Geochimica et Cosmochimica Acta*, 228, 157–189. <https://doi.org/10.1016/j.gca.2018.02.034>
- Babechuk, M. G., Kleinhanns, I. C., Reitter, E., & Schoenberg, R. (2018). Kinetic stable Cr isotopic fractionation between aqueous Cr (III)-Cl-H₂O complexes at 25°C: Implications for Cr (III) mobility and isotopic variations in modern and ancient natural systems. *Geochimica et Cosmochimica Acta*, 222, 383–405. <https://doi.org/10.1016/j.gca.2017.10.002>
- Bain, D. J., & Bullen, T. D. (2005). Chromium isotope fractionation during oxidation of Cr (III) by manganese oxides. *Geochimica et Cosmochimica Acta*, 69, S212.
- Bekker, A., Slack, J. F., Planavsky, N., Krapež, B., Hofmann, A., Konhauser, K. O., & Rouxel, O. J. (2010). Iron formation: The sedimentary product of a complex interplay among mantle, tectonic, oceanic, and biospheric processes. *Economic Geology*, 105(3), 467–508. <https://doi.org/10.2113/gsecongeo.105.3.467>
- Bonnand, P., James, R., Parkinson, I., Connelly, D., & Fairchild, I. (2013). The chromium isotopic composition of seawater and marine carbonates. *Earth and Planetary Science Letters*, 382, 10–20. <https://doi.org/10.1016/j.epsl.2013.09.001>
- Bratsch, S. G. (1989). Standard electrode potentials and temperature coefficients in water at 298.15 K. *Journal of Physical and Chemical Reference Data*, 18(1), 1–21. <https://doi.org/10.1063/1.555839>
- Buerge, I. J., & Hug, S. J. (1998). Influence of organic ligands on chromium (VI) reduction by iron (II). *Environmental Science & Technology*, 32(14), 2092–2099. <https://doi.org/10.1021/es970932b>
- Canfield, D. E., Zhang, S., Frank, A. B., Wang, X., Wang, H., Su, J., et al. (2018). Highly fractionated chromium isotopes in Mesoproterozoic-aged shales and atmospheric oxygen. *Nature Communications*, 9(1), 2871. <https://doi.org/10.1038/s41467-018-05263-9>

- Chovanec, P., Sparacino-Watkins, C. E., Zhang, N., Basu, P., & Stolz, J. (2012). Microbial reduction of chromate in the presence of nitrate by three nitrate respiring organisms. *Frontiers in Microbiology*, 3, 416.
- Cline, J. D., & Richards, F. A. (1972). Oxygen deficient conditions and nitrate reduction in the eastern tropical North Pacific Ocean. *Limnology and Oceanography*, 17(6), 885–900. <https://doi.org/10.4319/lo.1972.17.6.0885>
- Cole, D. B., Reinhard, C. T., Wang, X., Gueguen, B., Halverson, G. P., Gibson, T., et al. (2016). A shale-hosted Cr isotope record of low atmospheric oxygen during the Proterozoic. *Geology*, G37787, 37781.
- Connelly, D. P., Statham, P. J., & Knap, A. H. (2006). Seasonal changes in speciation of dissolved chromium in the surface Sargasso Sea. *Deep Sea Research Part I: Oceanographic Research Papers*, 53(12), 1975–1988. <https://doi.org/10.1016/j.dsr.2006.09.005>
- Cranston, R. (1983). Chromium in Cascadia Basin, northeast Pacific Ocean. *Marine Chemistry*, 13(2), 109–125. [https://doi.org/10.1016/0304-4203\(83\)90020-8](https://doi.org/10.1016/0304-4203(83)90020-8)
- Cranston, R., & Murray, J. (1978). The determination of chromium species in natural waters. *Analytica Chimica Acta*, 99(2), 275–282. [https://doi.org/10.1016/S0003-2670\(01\)83568-6](https://doi.org/10.1016/S0003-2670(01)83568-6)
- Crowe, S. A., Døssing, L. N., Beukes, N. J., Bau, M., Kruger, S. J., Frei, R., & Canfield, D. E. (2013). Atmospheric oxygenation three billion years ago. *Nature*, 501(7468), 535–538. <https://doi.org/10.1038/nature12426>
- Cutter, G., Andersson, P., Codispoti, L., Croot, P., Francois, R., Lohan, M., et al. (2010). Sampling and sample-handling protocols for GEOTRACES cruises. GEOTRACES.
- D'Arcy, J., Babechuk, M. G., Døssing, L. N., Gaucher, C., & Frei, R. (2016). Processes controlling the chromium isotopic composition of river water: Constrains from basaltic river catchments. *Geochimica et Cosmochimica Acta*, 186, 296–315. <https://doi.org/10.1016/j.gca.2016.04.027>
- Døssing, L., Dideriksen, K., Stipp, S., & Frei, R. (2011). Reduction of hexavalent chromium by ferrous iron: A process of chromium isotope fractionation and its relevance to natural environments. *Chemical Geology*, 285(1-4), 157–166. <https://doi.org/10.1016/j.chemgeo.2011.04.005>
- Eary, L. E., & Rai, D. (1987). Kinetics of chromium (III) oxidation to chromium (VI) by reaction with manganese dioxide. *Environmental Science & Technology*, 21(12), 1187–1193. <https://doi.org/10.1021/es00165a005>
- Economou-Eliopoulos, M., Frei, R., & Megremi, I. (2016). Potential leaching of Cr (VI) from laterite mines and residues of metallurgical products (red mud and slag): An integrated approach. *Journal of Geochemical Exploration*, 162, 40–49. <https://doi.org/10.1016/j.gexplo.2015.12.007>
- Elderfield, H. (1970). Chromium speciation in sea water. *Earth and Planetary Science Letters*, 9(1), 10–16. [https://doi.org/10.1016/0012-821X\(70\)90017-8](https://doi.org/10.1016/0012-821X(70)90017-8)
- Ellis, A. S., Johnson, T. M., & Bullen, T. D. (2002). Chromium isotopes and the fate of hexavalent chromium in the environment. *Science*, 295(5562), 2060–2062. <https://doi.org/10.1126/science.1068368>
- Emerson, S., Cranston, R., & Liss, P. (1979). Redox species in a reducing fjord: Equilibrium and kinetic considerations. *Deep Sea Research Part A. Oceanographic Research Papers*, 26(8), 859–878. [https://doi.org/10.1016/0198-0149\(79\)90101-8](https://doi.org/10.1016/0198-0149(79)90101-8)
- Fanning, J. C. (2000). The chemical reduction of nitrate in aqueous solution. *Coordination Chemistry Reviews*, 199(1), 159–179. [https://doi.org/10.1016/S0010-8545\(99\)00143-5](https://doi.org/10.1016/S0010-8545(99)00143-5)
- Farkaš, J., Frýda, J., Paulukat, C., Hathorne, E. C., Matoušková, Š., Rohovec, J., et al. (2018). Chromium isotope fractionation between modern seawater and biogenic carbonates from the Great Barrier Reef, Australia: Implications for the paleo-seawater $\delta^{53}\text{Cr}$ reconstruction. *Earth and Planetary Science Letters*, 498, 140–151. <https://doi.org/10.1016/j.epsl.2018.06.032>
- Fiedler, P. C., & Talley, L. D. (2006). Hydrography of the eastern tropical Pacific: A review. *Progress in Oceanography*, 69(2-4), 143–180. <https://doi.org/10.1016/j.pocean.2006.03.008>
- Frei, R., Gaucher, C., Poulton, S. W., & Canfield, D. E. (2009). Fluctuations in Precambrian atmospheric oxygenation recorded by chromium isotopes. *Nature*, 461(7261), 250–253. <https://doi.org/10.1038/nature08266>
- Frei, R., Paulukat, C., Bruggmann, S., & Kläbe, R. M. (2018). A systematic look at chromium isotopes in modern shells—Implications for paleo-environmental reconstructions. *Biogeosciences*. <https://doi.org/10.5194/bg-2018-5138>
- Frei, R., Poiré, D., & Frei, K. M. (2014). Weathering on land and transport of chromium to the ocean in a subtropical region (Misiones, NW Argentina): A chromium stable isotope perspective. *Chemical Geology*, 381, 110–124. <https://doi.org/10.1016/j.chemgeo.2014.05.015>
- Gilleaudeau, G., Frei, R., Kaufman, A., Kah, L., Azmy, K., Bartley, J., et al. (2016). Oxygenation of the mid-Proterozoic atmosphere: Clues from chromium isotopes in carbonates. *Geochemical Perspectives Letters*, 2, 178–187.
- Gilleaudeau, G. J., Voegelin, A. R., Thibault, N., Moreau, J., Ullmann, C. V., Kläbe, R. M., et al. (2018). Stable isotope records across the Cretaceous-Paleogene transition, Stevns Klint, Denmark: New insights from the chromium isotope system. *Geochimica et Cosmochimica Acta*, 235, 305–332. <https://doi.org/10.1016/j.gca.2018.04.028>
- Glass, J. B., Kretz, C. B., Ganesh, S., Ranjan, P., Seston, S. L., Buck, K. N., et al. (2015). Meta-omic signatures of microbial metal and nitrogen cycling in marine oxygen minimum zones. *Frontiers in Microbiology*, 6, 998.
- Goring-Harford, H. J., Klar, J., Pearce, C. R., Connelly, D. P., Achterberg, E. P., & James, R. H. (2018). Behaviour of chromium isotopes in the eastern sub-tropical Atlantic oxygen minimum zone. *Geochimica et Cosmochimica Acta*, 236, 41–59. <https://doi.org/10.1016/j.gca.2018.03.004>
- Gueguen, B., Reinhard, C. T., Algeo, T. J., Peterson, L. C., Nielsen, S. G., Wang, X., et al. (2016). The chromium isotope composition of reducing and oxic marine sediments. *Geochimica et Cosmochimica Acta*, 184, 1–19. <https://doi.org/10.1016/j.gca.2016.04.004>
- Holmden, C., Jacobson, A., Sageman, B., & Hurtgen, M. (2016). Response of the Cr isotope proxy to Cretaceous Ocean Anoxic Event 2 in a pelagic carbonate succession from the Western Interior Seaway. *Geochimica et Cosmochimica Acta*, 186, 277–295. <https://doi.org/10.1016/j.gca.2016.04.039>
- Hood, A., Planavsky, N. J., Wallace, M. W., & Wang, X. (2018). The effects of diagenesis on geochemical paleoredox proxies in sedimentary carbonates. *Geochimica et Cosmochimica Acta*, 232, 265–287. <https://doi.org/10.1016/j.gca.2018.04.022>
- Huang, J., Liu, J., Zhang, Y., Chang, H., Shen, Y., Huang, F., & Qin, L. (2018). Cr isotopic composition of the Laobao cherts during the Ediacaran–Cambrian transition in South China. *Chemical Geology*, 482, 121–130. <https://doi.org/10.1016/j.chemgeo.2018.02.011>
- Jeandel, C., & Minster, J. (1987). Chromium behavior in the ocean: Global versus regional processes. *Global Biogeochemical Cycles*, 1(2), 131–154. <https://doi.org/10.1029/GB001i002p00131>
- Karstensen, J., Stramma, L., & Visbeck, M. (2008). Oxygen minimum zones in the eastern tropical Atlantic and Pacific oceans. *Progress in Oceanography*, 77(4), 331–350. <https://doi.org/10.1016/j.pocean.2007.05.009>
- Kitchen, J. W., Johnson, T. M., Bullen, T. D., Zhu, J., & Raddatz, A. (2012). Chromium isotope fractionation factors for reduction of Cr (VI) by aqueous Fe (II) and organic molecules. *Geochimica et Cosmochimica Acta*, 89, 190–201. <https://doi.org/10.1016/j.gca.2012.04.049>

- Komori, K., Wang, P.-c., Toda, K., & Ohtake, H. (1989). Factors affecting chromate reduction in *Enterobacter cloacae* strain HO1. *Applied Microbiology and Biotechnology*, 31, 567–570.
- McClain, C., & Maher, K. (2016). Chromium fluxes and speciation in ultramafic catchments and global rivers. *Chemical Geology*, 426, 135–157. <https://doi.org/10.1016/j.chemgeo.2016.01.021>
- Moos S. B. (2018). The marine biogeochemistry of chromium isotopes. Ph.D. Dissertation, Massachusetts Institute of Technology. <https://doi.org/10.1575/1912/9489>
- Moos, S. B., & Boyle, E. A. (2018). Determination of accurate and precise chromium isotope ratios in seawater samples by MC-ICP-MS illustrated by analysis of SAFe station in the North Pacific Ocean. *Chemical Geology*. <https://doi.org/10.1016/j.chemgeo.2018.1007.1027>
- Murray, J. W., Spell, B., & Paul, B. (1983). The contrasting geochemistry of manganese and chromium in the eastern tropical Pacific Ocean. In *Trace Metals in Sea Water* (pp. 643–669). Boston, MA: Springer. https://doi.org/10.1007/978-1-4757-6864-0_37
- Nakayama, E., Tokoro, H., Kuwamoto, T., & Fujinaga, T. (1981). Dissolved state of chromium in seawater. *Nature*, 290(5809), 768–770. <https://doi.org/10.1038/290768a0>
- Nordstrom, D., Plummer, L., Wigley, T., Wolery, T., Ball, J. W., Jenne, E., et al. (1979). A comparison of computerized chemical models for equilibrium calculations in aqueous systems. In *Chemical Modeling in Aqueous Systems* (pp. 857–892). Washington, DC: American Chemical Society.
- Paulukat, C., Døssing, L. N., Mondal, S. K., Voegelin, A. R., & Frei, R. (2015). Oxidative release of chromium from Archean ultramafic rocks, its transport and environmental impact—A Cr isotope perspective on the Sukinda Valley ore district (Orissa, India). *Applied Geochemistry*, 59, 125–138. <https://doi.org/10.1016/j.apgeochem.2015.04.016>
- Paulukat, C., Gilleaudeau, G. J., Chernyavskiy, P., & Frei, R. (2016). The Cr-isotope signature of surface seawater—A global perspective. *Chemical Geology*, 444, 101–109. <https://doi.org/10.1016/j.chemgeo.2016.10.004>
- Pereira, N. S., Vögelin, A. R., Paulukat, C., Sial, A. N., Ferreira, V. P., & Frei, R. (2015). Chromium isotope signatures in scleractinian corals from the Rocas Atoll, Tropical South Atlantic. *Geobiology*, 4, 1–13.
- Planavsky, N. J., Reinhard, C. T., Wang, X., Thomson, D., McGoldrick, P., Rainbird, R. H., et al. (2014). Low Mid-Proterozoic atmospheric oxygen levels and the delayed rise of animals. *Science*, 346(6209), 635–638. <https://doi.org/10.1126/science.1258410>
- Qin, L., & Wang, X. (2017). Chromium isotope geochemistry. *Reviews in Mineralogy and Geochemistry*, 82(1), 379–414. <https://doi.org/10.2138/rmg.2017.82.10>
- Reinhard, C. T., Planavsky, N. J., Robbins, L. J., Partin, C. A., Gill, B. C., Lalonde, S. V., et al. (2013). Proterozoic ocean redox and biogeochemical stasis. *Proceedings of the National Academy of Sciences of the United States of America*, 110(14), 5357–5362. <https://doi.org/10.1073/pnas.1208622110>
- Reinhard, C. T., Planavsky, N. J., Wang, X., Fischer, W. W., Johnson, T. M., & Lyons, T. W. (2014). The isotopic composition of authigenic chromium in anoxic marine sediments: A case study from the Cariaco Basin. *Earth and Planetary Science Letters*, 407, 9–18. <https://doi.org/10.1016/j.epsl.2014.09.024>
- Richards, F. A. (1970). *Physical, chemical, and productivity data from a survey of the Caribbean Sea and the Northeastern Tropical Pacific Ocean*. University of Washington.
- Richard, F. C., & Bourg, A. C. (1991). Aqueous geochemistry of chromium: A review. *Water Research*, 25(7), 807–816. [https://doi.org/10.1016/0043-1354\(91\)90160-R](https://doi.org/10.1016/0043-1354(91)90160-R)
- Rodler, A., Sánchez-Pastor, N., Fernández-Díaz, L., & Frei, R. (2015). Fractionation behavior of chromium isotopes during coprecipitation with calcium carbonate: Implications for their use as paleoclimatic proxy. *Geochimica et Cosmochimica Acta*, 164, 221–235. <https://doi.org/10.1016/j.gca.2015.05.021>
- Rue, E. L., Smith, G. J., Cutter, G. A., & Bruland, K. W. (1997). The response of trace element redox couples to suboxic conditions in the water column. *Deep Sea Research Part I: Oceanographic Research Papers*, 44(1), 113–134. [https://doi.org/10.1016/S0967-0637\(96\)00088-X](https://doi.org/10.1016/S0967-0637(96)00088-X)
- Saad, E. M., Wang, X., Planavsky, N. J., Reinhard, C. T., & Tang, Y. (2017). Redox-independent chromium isotope fractionation induced by ligand-promoted dissolution. *Nature Communications*, 8(1), 1590. <https://doi.org/10.1038/s41467-017-01694-y>
- Schauble, E., Rossman, G. R., & Taylor, H. P. Jr. (2004). Theoretical estimates of equilibrium chromium-isotope fractionations. *Chemical Geology*, 205(1-2), 99–114. <https://doi.org/10.1016/j.chemgeo.2003.12.015>
- Scheiderich, K., Amini, M., Holmden, C., & Francois, R. (2015). Global variability of chromium isotopes in seawater demonstrated by Pacific, Atlantic, and Arctic Ocean samples. *Earth and Planetary Science Letters*, 423, 87–97. <https://doi.org/10.1016/j.epsl.2015.04.030>
- Schoenberg, R., Zink, S., Staubwasser, M., & von Blanckenburg, F. (2008). The stable Cr isotope inventory of solid Earth reservoirs determined by double spike MC-ICP-MS. *Chemical Geology*, 249(3-4), 294–306. <https://doi.org/10.1016/j.chemgeo.2008.01.009>
- Stramma, L., Schmidtko, S., Levin, L. A., & Johnson, G. C. (2010). Ocean oxygen minima expansions and their biological impacts. *Deep Sea Research Part I: Oceanographic Research Papers*, 57(4), 587–595. <https://doi.org/10.1016/j.dsr.2010.01.005>
- Sun, Z., Wang, X., & Planavsky, N. (2019). Cr isotope systematics in the Connecticut River estuary. *Chemical Geology*, 506, 29–39. <https://doi.org/10.1016/j.chemgeo.2018.12.034>
- Vatsouria, A., Vainshtein, M., Kusch, P., Wiessner, A., D, K., & Kaestner, M. (2005). Anaerobic co-reduction of chromate and nitrate by bacterial cultures of *Staphylococcus epidermidis* L-02. *Journal of Industrial Microbiology & Biotechnology*, 32(9), 409–414. <https://doi.org/10.1007/s10295-005-0020-0>
- Wang, X. L., Johnson, T. M., & Ellis, A. S. (2015). Equilibrium isotopic fractionation and isotopic exchange kinetics between Cr (III) and Cr (VI). *Geochimica et Cosmochimica Acta*, 153, 72–90. <https://doi.org/10.1016/j.gca.2015.01.003>
- Wang, X. L., Planavsky, N., Hull, P., Tripathi, A., Reinhard, C., Zou, H., et al. (2016). Chromium isotopic composition of core-top planktonic foraminifera. *Geobiology*, 1–14.
- Wang, X. L., Planavsky, N. J., Reinhard, C. T., Zou, H., Ague, J. J., Wu, Y., et al. (2016). Chromium isotope fractionation during subduction-related metamorphism, black shale weathering, and hydrothermal alteration. *Chemical Geology*, 429, 19–33.
- Wang, X. L., Reinhard, C., Planavsky, N., Owens, J. D., Lyons, T., & Johnson, C. M. (2016). Sedimentary chromium isotopic compositions across the Cretaceous OAE2 at Demerara Rise Site 1258. *Chemical Geology*, 429, 85–92. <https://doi.org/10.1016/j.chemgeo.2016.03.006>
- Wei, W., Frei, R., Kläbe, R., Li, D., Wei, G.-Y., & Ling, H.-F. (2018). Redox condition in the Nanhua Basin during the waning of the Sturtian glaciation: A chromium-isotope perspective. *Precambrian Research*, 319, 198–210. <https://doi.org/10.1016/j.precambres.2018.02.009>
- Wille, M., Nebel, O., van Kranendonk, M. J., Schoenberg, R., Kleinhanns, I. C., & Ellwood, M. J. (2013). Mo-Cr isotope evidence for a reducing Archean atmosphere in 3.46–2.76 Ga black shales from the Pilbara, Western Australia. *Chemical Geology*, 340, 68–76. <https://doi.org/10.1016/j.chemgeo.2012.12.018>
- Wright, J. J., Konwar, K. M., & Hallam, S. J. (2012). Microbial ecology of expanding oxygen minimum zones. *Nature Reviews Microbiology*, 10(6), 381–394. <https://doi.org/10.1038/nrmicro2778>